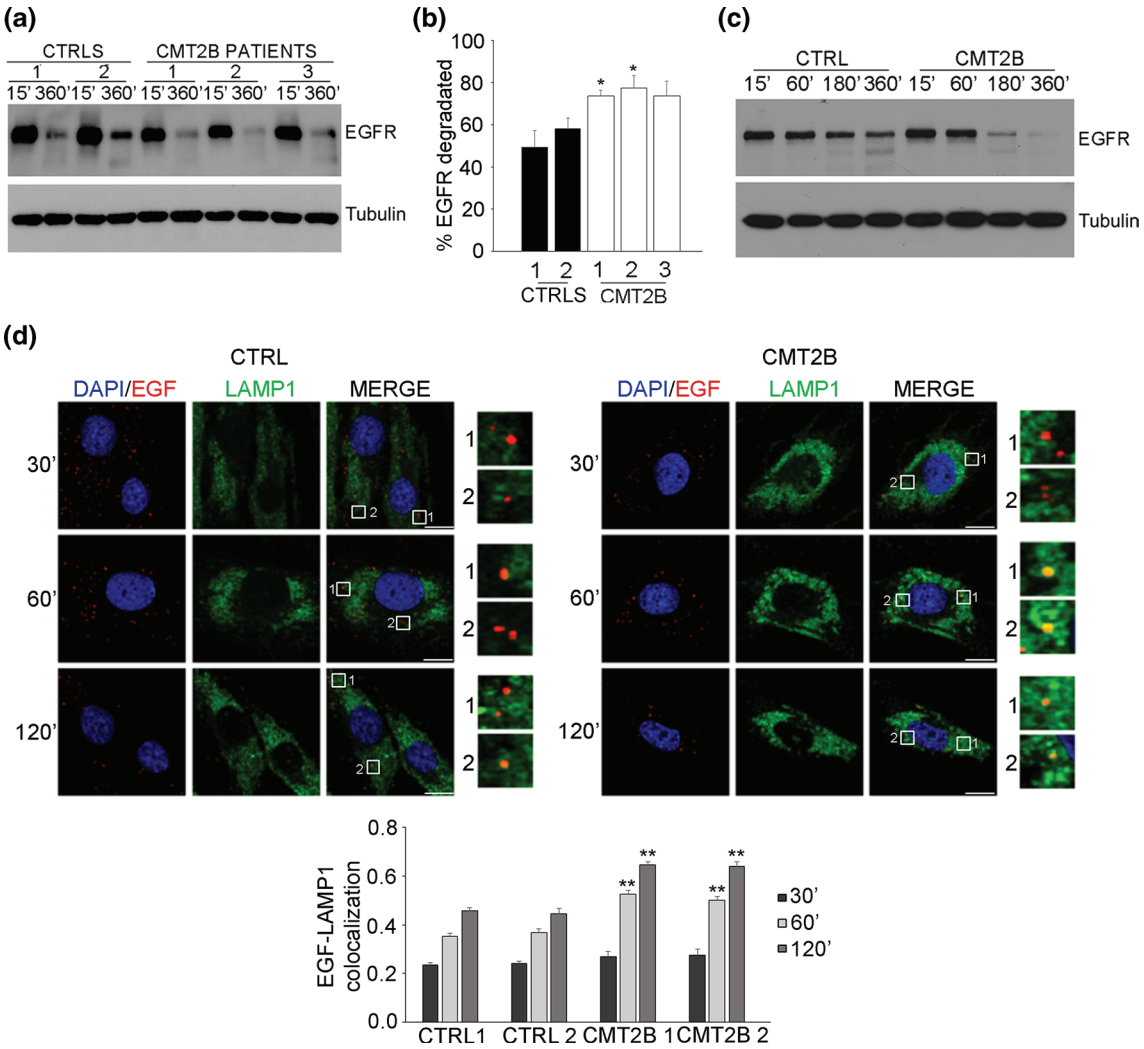

Fig. 5 Degradation activity is higher in CMT2B fibroblasts carrying the RAB7^{V162M} mutation. **a** Fibroblasts derived from two healthy individuals and three CMT2B patients were incubated with cycloheximide for 1 h and subsequently stimulated with EGF for 15 and 360 min. Cell lysates were analyzed by immunoblotting with antibody against EGFR and tubulin. **b** Densitometric analysis was performed with NIH ImageJ normalizing against tubulin. Statistical analysis was performed using Student's *t* test with control fibroblasts as referring sample. **c** Fibroblasts derived from control and CMT2B (patient 1) were incubated with cycloheximide for 1 h and subsequently stimulated with EGF for the indicated times. Cell lysates were analyzed by immunoblotting with antibody against EGFR and tubulin. **d** Skin fibroblasts derived from two healthy individuals and two CMT2B patients (patients 1 and 2) were incubated overnight in starvation medium and then incubated for 1 h at 4 °C with rhodamine-EGF. After several washing, cells were incubated in complete DMEM medium at 37 °C for 30 min, 1 h and 2 h and then fixed, permeabilized, immunolabeled with anti-LAMP1 followed by Alexa488-conjugated secondary antibody while nuclei were stained with DAPI. For each image, magnifications of the boxed areas are shown. Bars 10 μM. Data represent the mean ± SEM of at least 50 cells of three independent experiments. Statistical analyses were performed using Student's *t* test with control fibroblasts as referring sample. $^{**}p < 0.01$

AKT and ERK proteins in fibroblasts derived from three CMT2B patients and from two healthy individuals. Consistently with increased degradation of EGFR, we observed in CMT2B fibroblasts from the three patients a significant reduction in the activation of both AKT and ERK (Fig. 6a).

EGFR is also important for the regulation of cell motility [19, 49]. As we demonstrated that the RAB7^{V162M} mutation affects EGFR degradation and, as a consequence, inhibits AKT and ERK signaling, we hypothesized inhibition of cell migration. To measure cell migration, we performed a wound-healing assay. Control and CMT2B fibroblasts were grown to confluence, the cell layer was scratched and the wound area was monitored at different time intervals. Interestingly, we observed an approximately twofold increase in cell migration for CMT2B fibroblasts compared to control cells at 15 h after the scratch (Fig. 6b). Given this unexpected result, we investigated other players in cell migration.

RAC1, a Ras-related small GTPase involved in several cellular pathways, is a member of the RHO family that regulates actin cytoskeleton during cell motility [60]. In addition, during cell migration, RAC1 activity is regulated by RAB7 [61]. Therefore, we analyzed the abundance and activation of RAC1 in CMT2B fibroblasts. We did not detect any differences in RAC1 protein amount between the control and CMT2B cells (Fig. 6c). However, we observed a significant increase of GTP-bound active RAC1 in CMT2B cells compared to controls, demonstrating that in these cells RAC1 is more activated (Fig. 6c).

Matrix metalloproteinases (MMPs) comprise a family of endopeptidases that degrade extracellular proteins promoting cell migration [62] and RAC1 is a mediator of MMP-2 activation [63]. Therefore, we monitored MMPs activity by gelatin zymography in control and CMT2B fibroblasts. In the medium of CMT2B cells, we detected two bands with different intensity corresponding to inactive and active MMP-2 (Fig. 6d) while in control cells only the inactive band was present.

To investigate the mechanism leading to increased RAC1 activation in CMT2B patients, we evaluated the expression of ARHGEF6 and RACGAP1 [64, 65]. We did not observe any difference in RACGAP1 expression between control and CMT2B fibroblasts, while we found an increased expression of ARHGEF6 in CMT2B fibroblasts (Fig. 6e) that could explain the increased RAC1 activation in these cells.

Altogether, these data demonstrate that EGFR signaling and cell migration are affected in CMT2B fibroblasts.

CMT2B sensory neurons show higher lysosomal activity

To confirm the data obtained in fibroblasts we decided to evaluate the abundance of lysosomal markers and lysosomal functionality in iPSC-derived sensory neurons from two CMT2B patients carrying the $RAB7^{V162M}$ mutation compared to two healthy individuals. The iPS cells obtained from CMT2B patients and controls showed the expression of the expected markers of undifferentiated ES cells (Fig. 7a–c), as well as pluripotent differentiation capacity into the three germ layers in vitro and in vivo (Fig. 7d, Supplemental Fig. 1).

iPSC-derived sensory neurons were grown on Matrigel-coated coverslips and showed normal axon network formation and expected markers of sensory dorsal root ganglia neurons (Fig. 8a). Previous data indicated that expression of CMT2B-causing RAB7 mutant proteins caused inhibition of neurite outgrowth [40, 41]. To assess neurite outgrowth in iPSCs-derived sensory neurons from control and CMT2B patients, the young neurons were plated and analyzed using IncuCyte® S3 Live-Cell Analysis System for 6 days. Interestingly, CMT2B neurons showed reduced neurite extensions as compared to controls (Fig. 8b), confirming previous results obtained by transient expression of RAB7 mutant proteins.

When we investigated in these cells late endosomal and lysosomal markers, we found that CMT2B neurons showed a twofold higher expression of LAMP1, confirming previous data obtained on CMT2B skin fibroblasts (Fig. 9a). We then performed immunofluorescence analysis to evaluate distribution and abundance of LAMP1-positive organelles and we observed a similar distribution in the perinuclear region of LAMP1 in the control and CMT2B neurons. However, CMT2B neurons showed a stronger expression of LAMP1 that was quantified confirming the data obtained by Western blotting and indicating an increase of about two times (Fig. 9b). We next investigated the abundance of the mature form of cathepsin D and we found an increase in CMT2B patients, similar to what we observed in fibroblasts (Fig. 9c). As higher cathepsin D maturation correlates with higher lysosomal activity, we performed a DQ-Red BSA assay. As expected, CMT2B neurons display higher fluorescent DQ-BSA staining than control neurons indicating higher lysosomal activity. Quantification of DQ-Green BSA puncta revealed an increase of about fivefold (Fig. 9d).

Altogether, these results indicate that iPS-derived neurons from CMT2B patient show higher lysosomal activity.

Discussion

In this study, we demonstrate that late endocytic traffic is altered in CMT2B compared to control cells. In particular, we show that RAB9 and CI-MPR as well as lysosomal proteins such as LAMP1, LAMP2 and cathepsin D are more abundant in these cells and that lysosomes, more numerous in CMT2B cells compared to control, display increased activity (Fig. 10). Indeed, the activity of three lysosomal enzymes (cathepsin B, D and L) is increased as well as degradation of EGFR and DQ BSA (Fig. 10). These data are consistent with several studies demonstrating that alterations of endocytic traffic induce neurodegeneration [11, 66]. In fact, upregulation of RAB proteins involved in endocytic traffic occurs during the progression of a number of neurodegenerative disorders including Alzheimer's disease [67–70]. Furthermore, increased transport to endosomes of proteases, such as cathepsin B and L, coupled with higher expression of CI-MPR, was shown in Alzheimer's disease [68, 71]. Indeed, in neurodegenerative disorders, increased endocytic flux induces abnormal degradation of signaling complexes, impairing neurotrophin receptor signaling that, in turn, could be responsible for neurodegeneration.

We also found that, although the expression of early endocytic RABs is not altered in CMT2B cells, EAP30 (ESCRT-II member) and TSG101 (ESCRT-I member) levels were

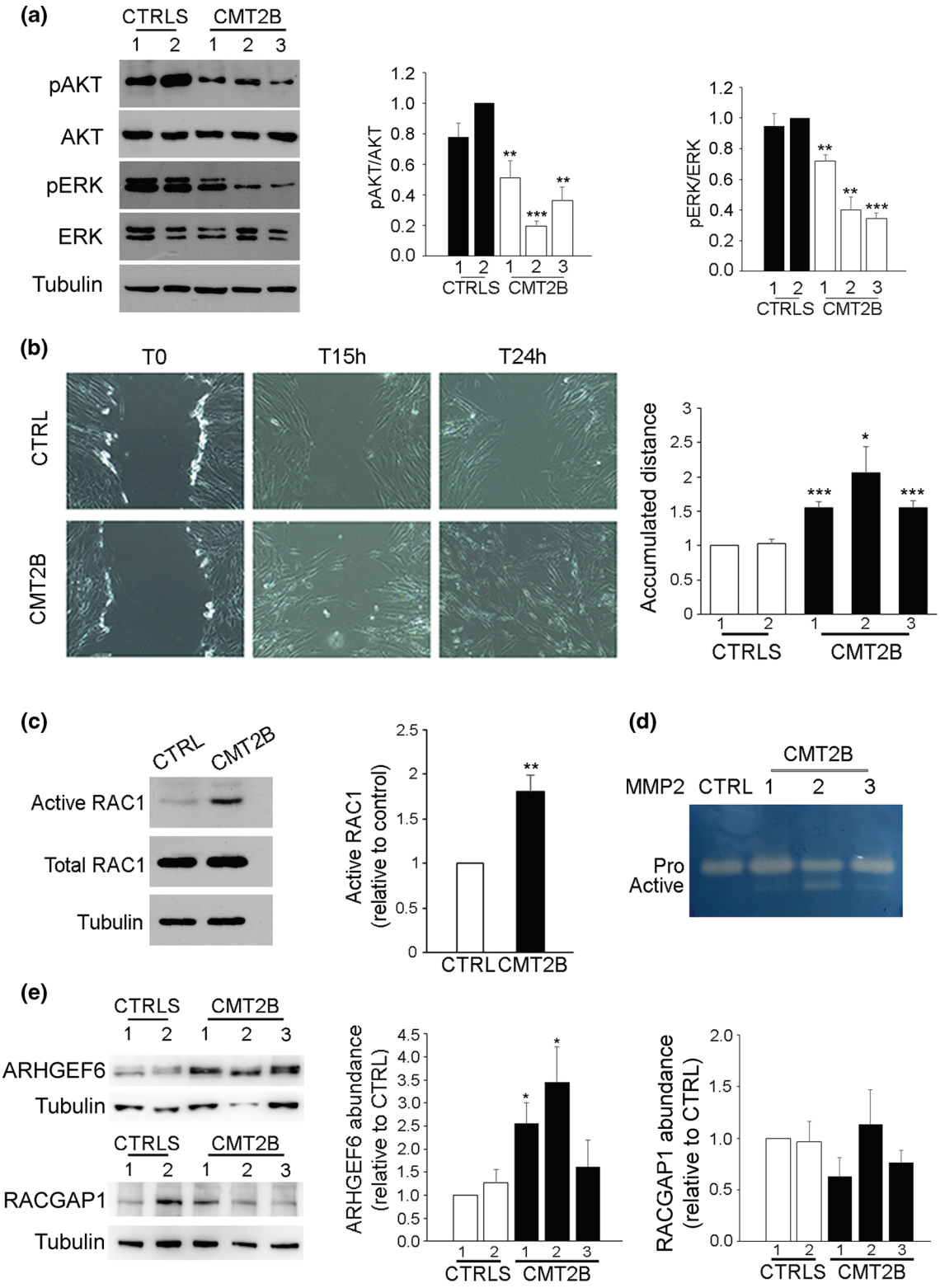

strongly reduced (Fig. 10). The reduction of ESCRT components in CMT2B cells is consistent with previously reported cargo-dependent degradation of ESCRT components [72–74]. Indeed, it was shown that ESCRT-I components are delivered together with the cargo to lysosomes, where they are degraded [74]. Thus, lower levels of TSG101 are indicative of increased utilization. Therefore, our data on increased lysosomal activity and increased EGFR degradation are in